Photosynthesis and Calcification by Emiliania huxleyi (Prymnesiophyceae) as a Function of Inorganic Carbon Species

Buitenhuis, Erik T.; Baar, Hein J.W. de; Veldhuis, Marcel J.W.

PHOTOSYNTHESIS AND CALCIFICATION BY *EMILIANIA HUXLEYI* (PRYMNESIOPHYCEAE) AS A FUNCTION OF INORGANIC CARBON SPECIES[1]

Erik T. Buitenhuis,[2] *Hein J. W. de Baar,*[2] *and Marcel J. W. Veldhuis*

Netherlands Institute for Sea Research, P.O. Box 59, 1790 AB Texel, The Netherlands

To test the possibility of inorganic carbon limitation of the marine unicellular alga *Emiliania huxleyi* (Lohmann) Hay and Mohler, its carbon acquisition was measured as a function of the different chemical species of inorganic carbon present in the medium. Because these different species are interdependent and covary in any experiment in which the speciation is changed, a set of experiments was performed to produce a multidimensional carbon uptake scheme for photosynthesis and calcification. This scheme shows that CO_2 that is used for photosynthesis comes from two sources. The CO_2 in seawater supports a modest rate of photosynthesis. The HCO_3^- is the major substrate for photosynthesis by intracellular production of CO_2 ($HCO_3^- + H^+ \rightarrow CO_2 + H_2O \rightarrow CH_2O + O_2$). This use of HCO_3^- is possible because of the simultaneous calcification using a second HCO_3^-, which provides the required proton ($HCO_3^- + Ca^{2+} \rightarrow CaCO_3 + H^+$). The HCO_3^- is the only substrate for calcification. By distinguishing the two sources of CO_2 used in photosynthesis, it was shown that *E. huxleyi* has a $K_{\frac{1}{2}}$ for external CO_2 of "only" 1.9 ± 0.5 μM (and a V_{max} of 2.4 ± 0.1 pmol·cell^{-1}·d^{-1}). Thus, in seawater that is in equilibrium with the atmosphere ($[CO_2] = 14$ μM, $[HCO_3^-] = 1920$ μM, at $fCO_2 = 360$ μatm, pH $= 8$, T $= 15°$ C), photosynthesis is 90% saturated with external CO_2. Under the same conditions, the rate of photosynthesis is doubled by the calcification route of CO_2 supply (from 2.1 to 4.5 pmol·cell^{-1}·d^{-1}). However, photosynthesis is not fully saturated, as calcification has a $K_{\frac{1}{2}}$ for HCO_3^- of 3256 ± 1402 μM and a V_{max} of 6.4 ± 1.8 pmol·cell^{-1}·d^{-1}. The H^+ that is produced during calcification is used with an efficiency of 0.97 ± 0.08, leading to the conclusion that it is used intracellularly. A maximum efficiency of 0.88 can be expected, as NO_3^- uptake generates a H^+ sink (OH^- source) for the cell. The success of *E. huxleyi* as a coccolithophorid may be related to the efficient coupling between H^+ generation in calcification and CO_2 fixation in photosynthesis.

Key index words: calcification rate; CO_2 (carbon dioxide); coccolithophorid; dissolved inorganic carbon system; *Emiliania huxleyi*; Haptophyta; HCO_3^- (bicarbonate); pH; photosynthetic carbon fixation

Abbreviations: CCM, carbon-concentrating mechanism; C/P, calcification rate/photosynthetic rate; DIC, dissolved inorganic carbon; fCO_2, fugacity of CO_2; μ, specific growth rate; POC/PON, particulate organic carbon/particulate organic nitrogen

Emiliania huxleyi is a coccolithophorid alga with a worldwide distribution. It usually forms blooms in the temperate regions after the spring diatom bloom. *E. huxleyi* produces coccoliths, or platelets of distinctive shape that are made of $CaCO_3$ in the mineral form of calcite. These are produced intracellularly by an energy-requiring process in specialized vesicles that are derived from the Golgi apparatus (Westbroek et al. 1989).
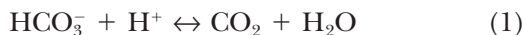
Several theories link the production of coccoliths to the success of *E. huxleyi* (Young 1994). As early as 1962, Paasche suggested that calcification and photosynthesis in *E. huxleyi* might be linked by a mechanism equivalent to the symbiosis of corals. By precipitating $CaCO_3$, it shifts the equilibrium of dissolved inorganic carbon (DIC) toward CO_2, which can be used in photosynthesis. Thus, calcification might represent an alternative to a carbon-concentrating mechanism (CCM) in decreasing photorespiration by the oxygenase activity of ribulose-bisphosphate-carboxylase-oxygenase (Rubisco). In view of the widespread occurrence of blooms of *E. huxleyi* (e.g. Brown and Yoder 1994), this mechanism might be more efficient than a CCM in using resources such as energy, PO_4^{3-} and/or Zn^{2+}. Anning et al. (1996) have shown the potential merit of calcification as an energy-efficient way of supplying Rubisco with CO_2, but the actual balance of the comparison with a CCM depends on the as yet unknown transport route of the ions involved. Although the competitive ability of *E. huxleyi* for PO_4^{3-} is well documented (Egge and Heimdal 1994), no mechanism to link this feature with calcification has been identified. Raven and Johnston (1991) have pointed out that an alga with a CCM would need more Zn^{2+} than an alga that depends on diffusive CO_2 entry. Calcification might represent an intermediate requirement of Zn^{2+} as a cofactor in the enzyme carbonic anhydrase (Morel et al. 1994).

The half-life time of the conversion of HCO_3^- into CO_2 is 38 s at 18° C (Wolf-Gladrow and Riebesell 1997). The inorganic carbon species that are incorporated into calcite and photosynthetic organic carbon have been investigated using this relatively long equilibration time (Sikes et al. 1980). The ^{14}C was added at nonequilibrium concentrations (as $^{14}CO_2$

or $H^{14}CO_3^-$), and its incorporation was measured during the time interval in which this ^{14}C equilibrated. It was found that ^{14}C added as HCO_3^- is preferentially incorporated into calcite, whereas CO_2 is preferentially incorporated into organic carbon. From these results it was concluded that inside the cell two HCO_3^- are split into CO_3^{2-} and CO_2. The CO_3^{2-} is precipitated as calcite ($CaCO_3$), and the CO_2 is fixed by the enzyme Rubisco to produce organic carbon (eqs. 1–3):

$$HCO_3^- + H^+ \leftrightarrow CO_2 + H_2O \tag{1}$$

$$HCO_3^- + Ca^{2+} \leftrightarrow CaCO_3 + H^+ \tag{2}$$

$$CO_2 + H_2O \leftrightarrow (CH_2O)_{organic} + O_2 \tag{3}$$

The conversion of HCO_3^- into CO_3^{2-} was not discussed. The half-life time is 77 ms at 18° C (Wolf-Gladrow and Riebesell 1997), and thus these experiments did not distinguish between HCO_3^- and CO_3^{2-}. The disequilibrium experiments with ^{14}C were confirmed with equilibrium ^{13}C discriminations in calcite and photosynthetic carbon (Sikes and Wilbur 1982). However, while the equilibrium discrimination between HCO_3^- and CO_2 is $-9.8‰$ at 18° C (Vogel et al. 1970, Mook et al. 1974), the equilibrium discrimination between HCO_3^- and CO_3^{2-} is only $-0.5‰$ at 18° C (Thode et al. 1965). Thus, this method did not adequately distinguish between HCO_3^- and CO_3^{2-} either. By contrast, foraminifera were reported to use CO_3^{2-} in calcification (Spero et al. 1997). In view of these uncertainties, we have looked in more detail at the finding of Paasche (1964) that *E. huxleyi* uses HCO_3^- rather than CO_3^{2-} for calcification.

Nimer et al. (1994) reported carbonic anhydrase in the chloroplasts of *E. huxleyi*. This suggests that carbonic anhydrase might convert HCO_3^- into CO_2 at the site of fixation by Rubisco and minimize diffusive loss of CO_2. Nimer et al. (1995) formulated a model of inorganic carbon use in which photosynthesis and calcification are linked to maintain intracellular pH.

We have adapted this model, which is based on the reviewed data on inorganic carbon acquisition by *E. huxleyi,* as represented in Figure 1. We have tested this model by growing *E. huxleyi* at varying conditions in the DIC system. The four main species in the DIC system are HCO_3^-, CO_3^{2-}, CO_2, and H^+ (the concentration of H_2CO_3 is very low and is included within CO_2; Weiss 1974). These are correlated by two dissociation constants, so there are two degrees of freedom in the system, and it is not possible to vary one while keeping all the others constant. Thus, we have performed a set of experiments in which, for each experiment, only one species of DIC was kept constant. The concentrations of the other species were calculated using the dissociation constants. The rates of photosynthesis and calcification were measured. The results are used to elu-
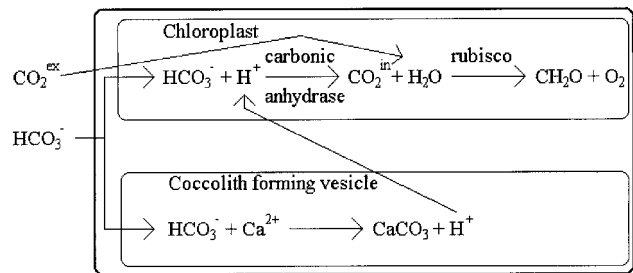

FIG. 1. Uptake of inorganic carbon by *Emiliania huxleyi* and mechanism of photosynthetic HCO_3^- use; CO_2^{ex} and CO_2^{in} represent the external and internal source of CO_2, respectively, that are used for photosynthesis. As explained in the Results section, these two sources were distinguished by performing several complementary experiments in the dissolved inorganic carbon system. Adapted after Nimer et al. (1995).

cidate the modes of inorganic carbon acquisition by *E. huxleyi*.

Although the geographic distribution of *E. huxleyi* has a wider temperature range, major blooms tend to occur in waters between about 10° C and 20° C (Brown and Yoder 1993). Thus, we have used a uniform 15° C in our experiments as being representative of bloom conditions. This corresponds with $CO_2 = 14$ μM and $HCO_3^- = 1920$ μM for oceanic conditions when CO_2 is in equilibrium with the atmosphere ($fCO_2 = 360$ μatm at pH $= 8$).

MATERIALS AND METHODS

Emiliania huxleyi strain Ch 24-90 (morphotype A, isolated from the North Sea; van Bleijswijk et al. 1991; characterized by van Bleijswijk et al. 1994) was adapted to the culture media in dilution cultures under nutrient-replete and light-saturated conditions. The media contained varying concentrations of HCO_3^-, CO_3^{2-}, CO_2, and H^+.

In each of four experiments, one species in the DIC system was kept constant while the others varied. The four species are H^+ expressed as pH, CO_3^{2-}, alkalinity, and CO_2. Alkalinity is the titer of the weak bases (Dickson 1981):

$$\text{Alkalinity} = [HCO_3^-] + 2 \cdot [CO_3^{2-}] + \text{minor constituents} \tag{4}$$

The experiment at constant CO_2 was performed twice, and the results are presented as average values. Except in the experiment at constant CO_2, the CO_2 concentrations were ⅛, ¼, ½, ¾, 1, and 2 times ambient (13.8 μM, or $fCO_2 = 360$ μatm). In the experiment at constant CO_2, the CO_3^{2-} concentrations were ⅛, ¼, ½, 1, 2, and 4 times ambient (123 μM). Dissolved inorganic carbon is the main pH buffer in seawater. However, the conditions in the experiments were chosen in such a way that the pH varied only between 7.5 and 8.5. Over this range, Paasche (1964) found no indication of a direct pH effect on carbon uptake by *E. huxleyi*. Speciation of the DIC system was calculated with the dissociation constants of Roy et al. (1993). The calculated concentrations of CO_2, HCO_3^-, and CO_3^{2-} in each medium are presented in Figure 2. The DIC to be added was calculated as the final DIC concentration $- 13.8$ μM (the DIC concentration after removal of HCO_3^- and CO_3^{2-}; see the following discussion). Speciation of the DIC system was calculated on the total pH scale (pH_T). The pH was adjusted on the NBS scale (pH_{NBS}). To correct for the residual liquid junction potential across the pH electrode in the dilute NBS buffers, 0.05 pH unit was subtracted from the pH_T (Bates 1975).

The medium was based on natural low-nutrient seawater with additions of 250 μM NO_3^-, 25 μM PO_4^{3-}, vitamins according to Paasche (1964), and trace metals to Guillard (1975).
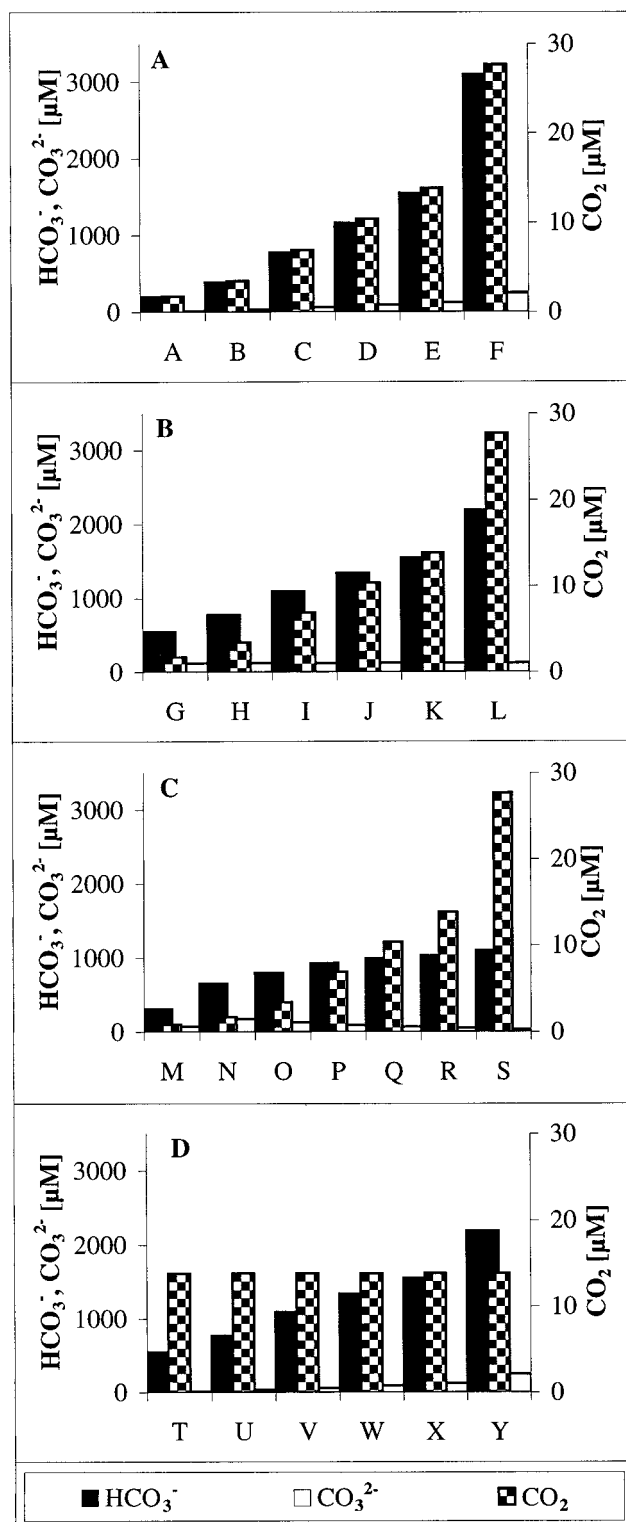
FIG. 2. Concentrations of dissolved inorganic carbon species in the experiments. Black areas, HCO_3^-; white areas, CO_3^{2-}; blocked bars, CO_2. (a) At a constant pH of 8.0. (b) At a constant CO_3^{2-} concentration of 123 μM. (c) At a constant alkalinity of 1214 μequivalents·L^{-1} (condition M: 661 μequivalents·L^{-1}). (d) At a constant CO_2 concentration of 13.8 μM.

The HCO_3^- and CO_3^{2-} were removed by addition of HCl to a concentration of 2.4 mM and bubbling with air overnight. After that the DIC was adjusted with 0.2 M $NaHCO_3$. The pH was adjusted with 0.1 M NaOH. Thus, there always was an adequate supply of nutrients except C.

Cells were grown at 15° C in a 16:8 h LD (light:dark) cycle with 300 μmol photons·$m^{-2}·^{-1}$ of fluorescent light on a rotating shaker at 120 rpm in serum bottles with a small headspace. Cells were precultured in the medium for 3 to 5 days and were then maintained at about 100,000 cells·mL^{-1} by diluting them 1.5- to 3-fold every day for 5 or 6 consecutive days. Dilutions of the cultures with a low fugacity of CO_2 (fCO_2, which is the partial pressure, corrected for the nonideal behavior of the gas mixture; Weiss 1974) were performed in a glove bag filled with synthetic air containing either 61 or 162 ppm CO_2. Headspaces of the media and the cultures with an fCO_2 of 360 μatm or 720 μatm were replaced with pressurized air and synthetic air containing 706 ppm CO_2, respectively, after each dilution. For the experiment at constant CO_2, the media were bubbled with pressurized air for 16 h prior to the experiment and for a few minutes after each dilution.

The rates of photosynthetic carbon incorporation and calcification were determined in triplicate with the microdiffusion technique according to Paasche and Brubak (1994) with some adaptations. Briefly, the method entails incubation of the cells with $DI^{14}C$, then filtering and washing with unlabeled seawater, and then separating the calcite carbon from the organic carbon by dissolving the calcite in H_3PO_4 and trapping the liberated $^{14}CO_2$ into a filter wetted with NaOH in a closed scintillation vial and counting the two fractions separately. The adaptations were that 60 mL of cell suspension was incubated with 37 kBq of $NaH^{14}CO_3$ for 24 h to measure over a full LD cycle. Incubations were started after the daily dilution at the end of the dark period. Subsamples of 1 mL were used without Carbo-sorb for determining the specific activity of the medium. Cultures were filtered onto 25-mm-diameter Whatman GF/F filters. No carrier solution was used, as this was not needed to make the filters adhere to the wall of the scintillation vials. The concentration of the 30 μL of NaOH for trapping the calcite carbon was only 5 M, as 12.5 M NaOH resulted in an unclear solution with the scintillation fluid (Instagel plus). This also gave a full transfer (96 $\pm$ 1%, n = 3). After addition of scintillation fluid, the samples were stored in the dark for at least 16 h before counting. Counting efficiency (by channels ratio) was between 80% and 87%. The average standard deviation for triplicate samples was 21% for the organic and calcite fractions and 10% for the medium. All reported errors are standard deviations. Error bars in the figures are the standard deviations of the numerators.

Cells were counted in triplicate using flow cytometry. Samples were taken at the end of the dark period, before the ^{14}C incubations, and after 24 h from cultures run in parallel to the ^{14}C incubations. Samples were preserved by addition of 0.36% formalin, buffered with 0.2% hexamine, and stored at $-20°$ C. Samples were thawed in tepid water before analysis. The flow rate was calibrated with 3-μm beads. The average standard deviation for triplicate cell counts was 3.5%. Specific growth rates were calculated as $\ln(N_{t=24}) - \ln(N_{t=0})$. The ^{14}C incorporation rates were expressed on the basis of the cell numbers at the beginning of the incubations.

Duplicate samples of 45 mL were filtered onto precombusted 11-mm-diameter GF/F glass filters at a vacuum of 0.2 bar. Samples were taken from unlabeled incubations run in parallel with the ^{14}C incubations. These were stored in the dark for 4 to 6 h following the end of the dark period before sampling. In some experiments these samples were analyzed for particulate organic carbon (POC) and particulate organic nitrogen (PON) with a Carlo Erba 1500NA series 2 NCS analyzer according to Verardo et al. (1990). In the other experiments these samples were analyzed for $\delta PO^{13}C$ and $\delta Ca^{13}CO_3$. The latter results will be presented in a separate paper.

Calculations of $K_{1/2}$ and V_{max} were performed using a Michaelis–Menten kinetics model,

$$\text{rate} = \frac{[\text{substrate}] \cdot V_{max}}{[\text{substrate}] + K_{1/2}} \qquad (5)$$

or equation 7 (see Results). This was preferred over a linearization of the data (such as the one of Lineweaver-Burk), as a direct fit to the model equation gives equal weight to all data points and allows the calculation of errors for the fitted parameters (J. van der Meer, pers. comm.)

RESULTS

Constant pH. At a constant pH of 8.0, the increasing concentrations of CO_2, HCO_3^-, and CO_3^{2-} are proportional to each other (Fig. 2a). The results show that *Emiliania huxleyi* becomes carbon limited over the range of concentrations tested (Fig. 3a–c). Because the species in the DIC system are interdependent, it cannot be proven that pH has no direct effect on carbon assimilation. However, the opposite trends with pH that are observed between Figure 3h, l, p shows that at least any effect of pH on the rates of photosynthesis and calcification is smaller than the effect of the other species; hereafter we assume that pH has no direct effects between 7.5 and 8.5.

Calcification stops at low DIC concentrations, whereas photosynthesis continues at a reduced rate (Fig. 3a–c). In fact, calcification does not show the typical saturation curve, in which the initial rate of increase is highest, as is observed for the photosynthetic rates. This does not mean that calcification and photosynthesis compete for inorganic carbon, as it can be calculated from the chemical speciation of the DIC system that calcification increases the availability of CO_2 for photosynthesis. When the rate of photosynthesis is fitted to a Michaelis–Menten kinetics equation, the $K_{1/2}$ is 7.5 ± 4.4 μM CO_2. However, by fitting photosynthesis to CO_2 alone, the increase of photosynthesis with HCO_3^- is ignored (see the following discussion).

Constant CO_3^{2-}. At a constant CO_3^{2-} concentration of 123 μM and with an increase in DIC, CO_2 increases faster than HCO_3^- (Fig. 2b). Opposite trends in carbon assimilation rates as a function of CO_3^{2-} are observed between Figure 3k and Figure 3c, o for both photosynthesis and calcification. This shows that CO_3^{2-} is not the substrate for either photosynthesis or calcification.

Constant alkalinity. At a constant alkalinity of 1214 μeq·L^{-1} and with increasing concentrations of CO_2 and HCO_3^-, the concentration of CO_3^{2-} decreases (conditions N–S in Fig. 2c). An additional condition was set up in which the concentrations of CO_2, HCO_3^-, and CO_3^{2-} were all lower (condition M in Fig. 2c; alkalinity = 661 μeq·L^{-1}). There is an increase in the calcification rate with HCO_3^- (Fig. 3j), whereas no trend is seen with CO_3^{2-} (Fig. 3k). The same increase in the calcification rate with HCO_3^- is observed in the other experiments (Figs. 3b, f, n, 5b). This clearly shows that for *E. huxleyi,* HCO_3^- is the substrate for calcification.

Constant CO_2. At a constant CO_2 concentration of 13.8 μM and an increase in DIC, the concentration

of CO_3^{2-} increases faster than the concentration of HCO_3^- (Fig. 2d). Photosynthesis increases with HCO_3^- (Fig. 3n). The increase is proportional to the increase in calcification rate (Figs. 3n, 4). This is consistent with the model for DIC uptake by *E. huxleyi* (Fig. 1), which would mean that it uses the protons that are generated by calcification to form CO_2 (eqq. 1, 2) and uses this extra CO_2 for photosynthesis (eq. 3). The tight coupling between the production of protons in calcification and the fixation of the generated CO_2 in photosynthesis can be seen from Figure 4. The equation for the line is

$$\text{Photosynthesis} = \text{Calcification} \times \text{efficiency}$$
$$+ \text{intercept} \qquad (6)$$

The efficiency with which the protons are used is 0.97 ± 0.08, and the extrapolated rate of photosynthesis at a calcification rate of 0 pmol·cell^{-1}·day^{-1} (intercept) is 2.07 ± 0.17 pmol·cell^{-1}·day^{-1} (n = 36).

In this experiment, again there was a minimum concentration of HCO_3^- required for calcification. This indicates that CO_2 is not a substrate for calcification because CO_2 was constantly high at the air-saturated concentration of 13.8 μM.

C/P and POC/PON ratios. The calcification/photosynthesis ratio (C/P, right-hand scales in Fig. 3) shows the best correlation with alkalinity (Fig. 5a). This reflects the fact that at constant CO_2, the C/P ratio increases with HCO_3^- because the calcification rate increases faster than photosynthesis (Fig. 3n) and that at constant HCO_3^-, the C/P ratio decreases with CO_2 (data not shown) because the photosynthetic rate increases with CO_2, whereas the calcification is not a function of CO_2. Qualitatively, alkalinity reacts in the same way.

The particulate POC/PON ratios were independent of the concentrations of CO_2, HCO_3^-, and CO_3^{2-} and of pH (data not shown). The average POC/PON ratio was 7.4 ± 1.1.

Michaelis–Menten kinetics. The CO_2 fixed during photosynthesis originates from two sources. One source is the external CO_2 in the seawater medium, and the other source is the internal CO_2 that is generated by calcification (CO_2^{ex} and CO_2^{in} in Fig. 1). In the experiment, at constant ambient CO_2 the external source was kept constant, and indeed the difference between photosynthesis and calcification was fairly constant as well (2.0 ± 0.4 pmol·cell^{-1}·day^{-1}). Using this finding, we have calculated the rate of photosynthesis that is supported by the external CO_2 as the difference between total photosynthesis and calcification. We have plotted this part of the photosynthesis as a function of the external concentration of CO_2. Fitting a Michaelis–Menten kinetics curve through these data gives a $K_{1/2}$ of 1.9 ± 0.5 μM CO_2 and a V_{max} of 2.4 ± 0.1 pmol·cell^{-1}·day^{-1} (Fig. 5b).

At low HCO_3^- concentrations, the calcification

stopped. This was seen both in the measurements of the calcification rates (Fig. 5c) and in the side-scatter characteristics of the cells in the flow cytometer (data not shown). The calcification rate was independent of the carbonate concentration (Fig. 3c, k, o), indicating that undersaturation of the seawater medium with respect to calcite was not the determining factor in preventing calcification. Thus, the calcification rate was fitted to a modified Michaelis–Menten equation in which a minimum HCO_3^- concentration for calcification was included:

$$\text{calcification rate} = \frac{(HCO_3^- - MIN_{HCO_3^-}) \cdot V_{max}}{(HCO_3^- - MIN_{HCO_3^-}) + K_m} \quad (7)$$

The results of this fit are MIN HCO_3^- = 506 ± 74 μM, K_m = 2750 ± 1328 μM, and V_{max} = 6.4 ± 1.8 pmol·cell^{-1}·day^{-1}. The HCO_3^- concentration at which half of V_{max} is reached is $K_{1/2}$ = K_m + MIN HCO_3^- = 3256 μM.

Despite the fact that the calcification rate was not dependent on the carbonate concentration, it was possible to fit the results to a Michaelis–Menten kinetics curve with a V_{max} of 6.6 ± 1.7 pmol·cell^{-1}·day^{-1} and a $K_{1/2}$ of 488 ± 179 μM (Fig. 5d). This fortuitous result is caused by the partial correlation between HCO_3^- and CO_3^{2-}, as is explained in the Discussion section.

Combining the calculated rates of photosynthesis on both the external CO_2 in the seawater and the internal CO_2 generated from HCO_3^- by calcification gives the total rate of photosynthesis as a function of both CO_2 and HCO_3^- (Fig. 6).

Specific growth rates. The specific growth rate (μ) was a function of both CO_2 and HCO_3^- (Fig. 7a, b). Growth rate was approximately half maximal both at low CO_2 and at low HCO_3^-, indicating that either substrate contributed about equally to the growth rate. We were unable to get a meaningful fit for the separate contributions of the two substrates. This was caused in the first place by a lack of data on the separate contributions of photosynthesis and calcification to the growth rate. A fit with separate $K_{1/2}$'s and $μ_{max}$'s for CO_2 and HCO_3^- gave a negative contribution of HCO_3^-. Fitting the data to the DIC concentration gave a $μ_{max}$ = 1.1 ± 0.1·day^{-1} and a $K_{1/2}$ = 270 ± 169 μM (Fig. 7c); however, as noted for the fit of the photosynthetic rate as a function of CO_2 (or DIC) at constant pH, this result is likely to be influenced by the average ratio of CO_2 to HCO_3^- in the experiments.

DISCUSSION

The described experiments under saturation of light and all nutrients except C confirm that calcification enhances photosynthetic carbon uptake, presumably through intracellular formation of CO_2. The $K_{1/2}$ of photosynthesis that was reported by Raven and Johnston (1991) based on data of Paasche (1964) was 9 μM CO_2. This was calculated from ex-periments conducted at constant pH, and thus it incorporates the increase in photosynthesis due to all inorganic carbon species and not just CO_2. If we follow the same method of calculation, we arrive at a similar $K_{1/2}$ of 7.5 ± 4.4 μM CO_2.

The present set of experiments in the DIC system indicates that the $K_{1/2}$ for photosynthesis that is calculated in this way depends on both CO_2^{ex} and HCO_3^-. Thus, the calculated $K_{1/2}$ does not describe the dependence of photosynthetic carbon fixation on the CO_2 concentration but also depends on the pH at which the experiment is performed. By separating the contributions of CO_2 and HCO_3^-, we found a $K_{1/2}$ of 1.9 μM for CO_2 and a $K_{1/2}$ of 3256 μM for HCO_3^-.

The published half-saturating CO_2 concentrations ($K_{1/2}$) for other algae (e.g. Raven and Johnston 1991: table 1) might also be subject to the reinterpretation that is presented here for *Emiliania huxleyi*. When the influence of CO_2 has not been separated from the influence of the other parameters of the DIC system, the published $K_{1/2}$'s will incorporate these influences for those algae that do not solely use CO_2. Thus, these $K_{1/2}$'s will depend on the experimental setup that was used to determine them. The experiments described here can also be used as an alternate procedure for determining whether algae can use HCO_3^- (or CO_3^{2-}), which might be preferable to using extremely high pH or estimating diffusive fluxes of CO_2 toward the cell.

The fact that the $K_{1/2}$ for HCO_3^- is much higher than the $K_{1/2}$ for CO_2 can be partially explained by the lower pH inside the cell, which reduces the intracellular abundance of HCO_3^- relative to CO_2. However, at a pH change across the cell membrane from 8 to 7 (Brownlee et al. 1995), the relative abundances change by a factor of 10 only as opposed to the ratio in the $K_{1/2}$'s of 1687. Apparently, there is a large difference in affinity between CO_2 and HCO_3^-. The difference in affinity by a factor of 169 is subject to some uncertainty, as the $K_{1/2}$ for HCO_3^- is poorly constrained. The reason for this is that, because of the narrow pH range that was chosen (see Materials and Methods), the HCO_3^- concentrations did not become high enough to observe the level part of the Michaelis–Menten curve that defines V_{max}. We can show the extent of this uncertainty by recalculating $K_{1/2}$ under the assumption that calcification is saturated at the highest HCO_3^- concentration of 3096 μM. Refitting the data with a V_{max} of 3.1 pmol·cell^{-1}·day^{-1}, we calculated a MIN HCO_3^- = 576 ± 35 μM and K_m = 724 ± 84 μM. This gives a $K_{1/2}$ of 1300 μM, which is still a factor 674 higher than the $K_{1/2}$ for CO_2. Thus, the affinity of the cell for CO_2 appears to be at least 67 times larger than the affinity for HCO_3^-.

Calcification stops below a certain HCO_3^- concentration (Fig. 5b). Below this MIN HCO_3^-, the cells are apparently unable to realize a concentration product of Ca^{2+} and CO_3^{2-} above the saturation
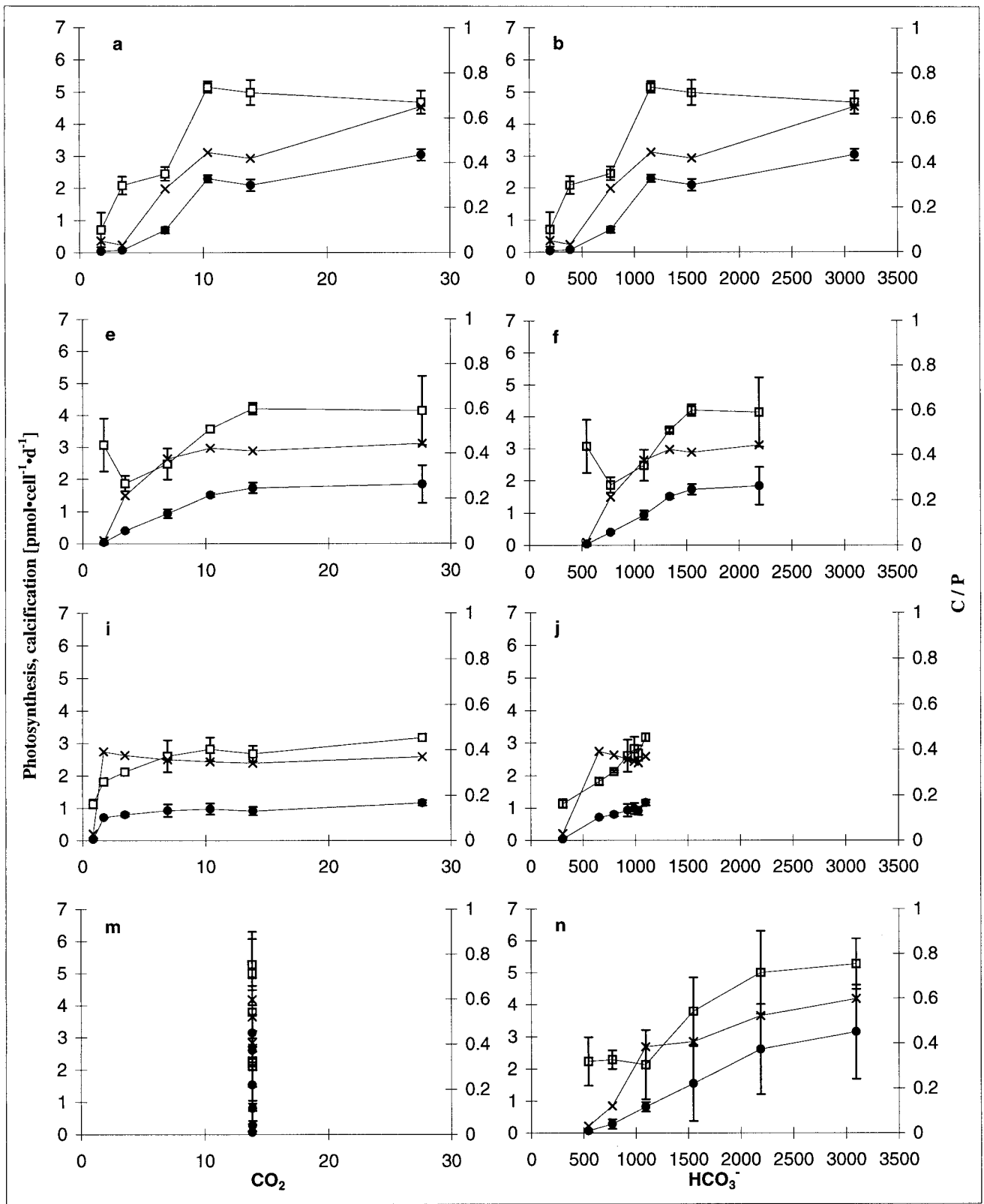
FIG. 3.   Rates of ^{14}C incorporation. Left y-axis: □ photosynthetic rates (P), ● calcification rates (C). Right y-axis: × C/P ratios (cal-cification/photosynthesis). (a–d) At constant pH. (e–h) At constant CO_3^{2-}. (i–l) At constant alkalinity. (m–p) At constant CO_2. Error bars indicate standard deviations (a–l: n = 3; m–p: average of two experiments, n = 6).
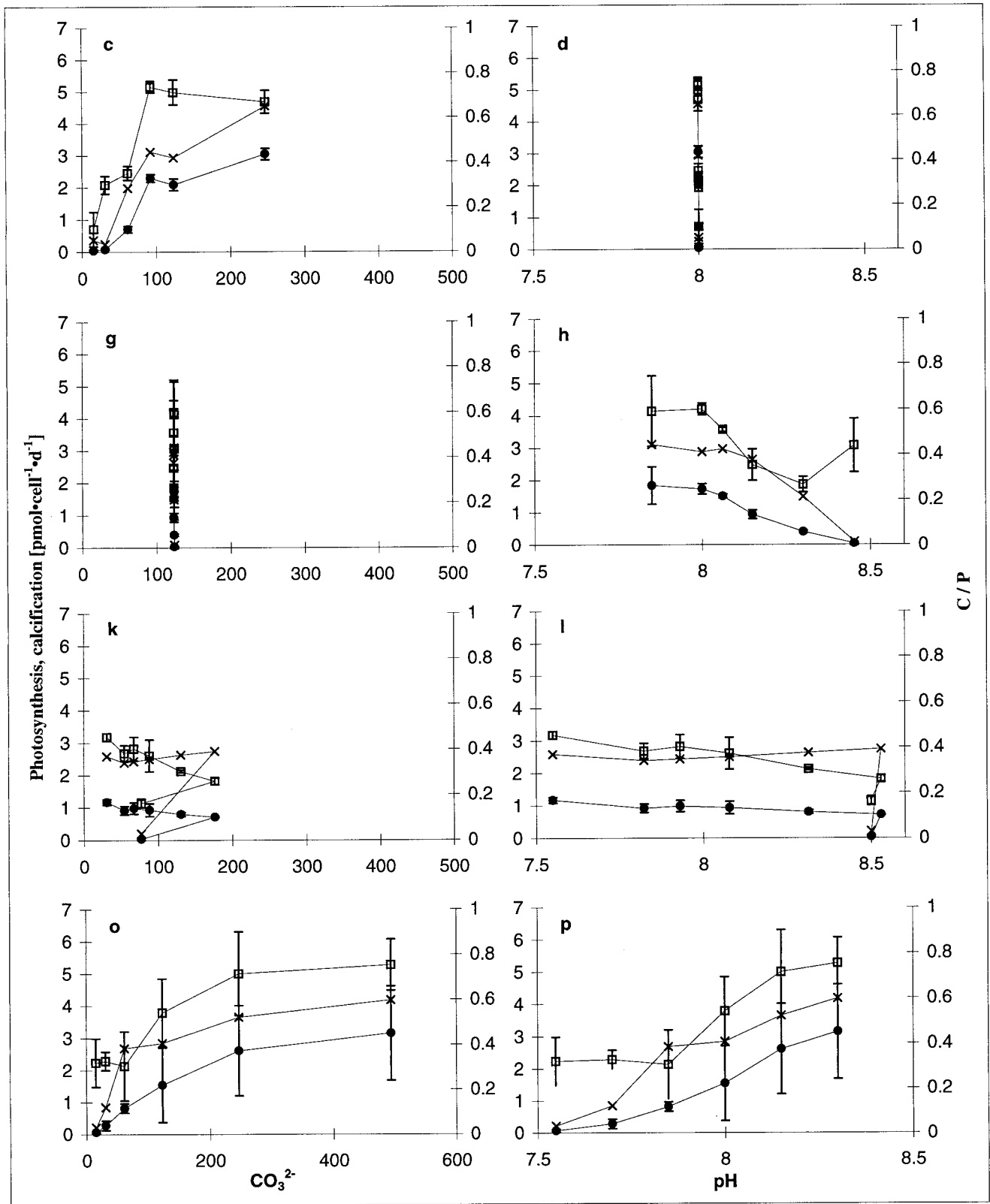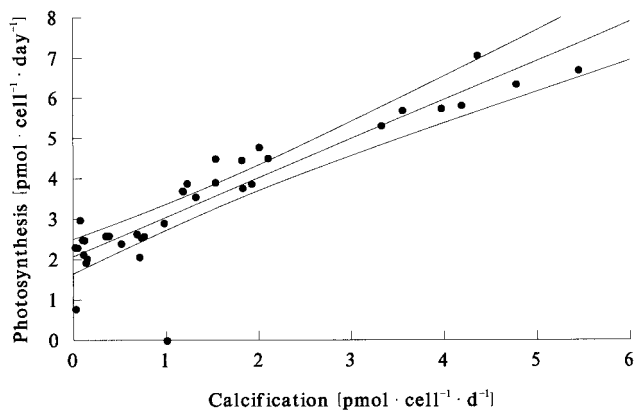
FIG. 3. Continued.

FIG. 4. Rate of photosynthetic carbon incorporation as a function of calcification rate, fitted by linear regression with 95% confidence levels shown. Results are from the two experiments (12 cultures) at constant CO_2. For parameter values, see text.

FIG. 6. Photosynthetic rates as a function of CO_2 and HCO_3^-. The plotted three-dimensional function is the sum of the functions plotted in Figures 5a, b. Filled circles represent experimental data points; open circles represent the corresponding calculated photosynthetic rates that lie on the surface of the function. Note that below $[HCO_3^-] = 506$ μM, the calcification rate is zero and that photosynthesis depends solely on CO_2.

point within the coccolith-forming vesicle. Calcification did not depend on the CO_3^{2-} concentration in the medium, so we can tentatively conclude that the pH in the coccolith forming vesicle depends on the transport of HCO_3^- across the cell membrane. Brownlee et al. (1995) measured the cytosolic pH of *E. huxleyi* and found an increase from 6.3 to 7.0 on addition of DIC to DIC-starved cells. They suggested that HCO_3^- might act as an intracellular pH buffer. In the coccolith-forming vesicles, the HCO_3^- might buffer the acidic polysaccharides that control the precipitation of calcite.

In the experiments at constant CO_3^{2-} and constant alkalinity, it was shown that HCO_3^- and not CO_3^{2-} is the substrate for calcification (Fig. 3f, g, j, k). This confirms the results of Paasche (1964) and shows

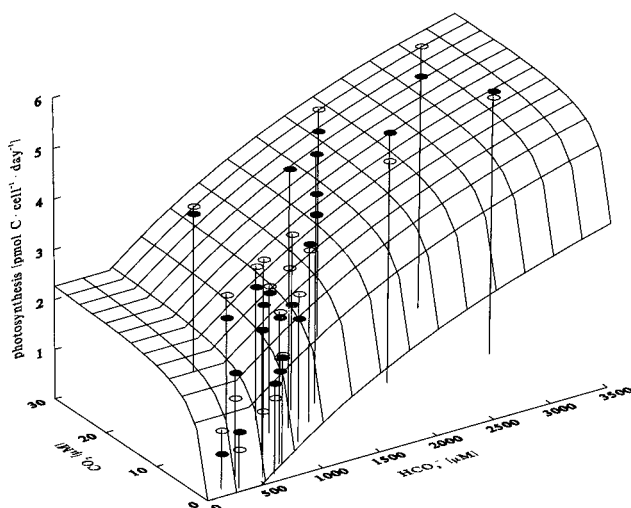that calcification in the plant *E. huxleyi* is different from that in the animal foraminifera (cf. Spero et al. 1997).

Despite the fact that HCO_3^- is the substrate for calcification, a positive correlation was still seen between the calcification rate and CO_3^{2-} (Fig. 5c) because a bias occurred in the experiments toward a correlation of HCO_3^- and CO_3^{2-}. This bias is caused by the speciation of the DIC system. At constant pH, the concentrations of HCO_3^- and CO_2 both in-

FIG. 5. (a) Part of the photosynthetic rate that is supported by CO_2 from the medium (photosynthesis–calcification) fitted to Michaelis–Menten kinetics, equation 5 (excluding condition 1 at constant carbonate, indicated by ×). (b) Calcification rate as a function of HCO_3^- fitted to equation 7 (excluding the points below $MIN_{HCO_3^-}$, indicated by ×). (c) Calcification rate as a function of CO_3^{2-}. ▼ constant pH, ☆ constant CO_2, + constant CO_3^{2-}, □ constant alkalinity conditions 1–6, ■ constant alkalinity condition 0. Curve fitted to Michaelis–Menten kinetics using all data points. For parameter values, see text.
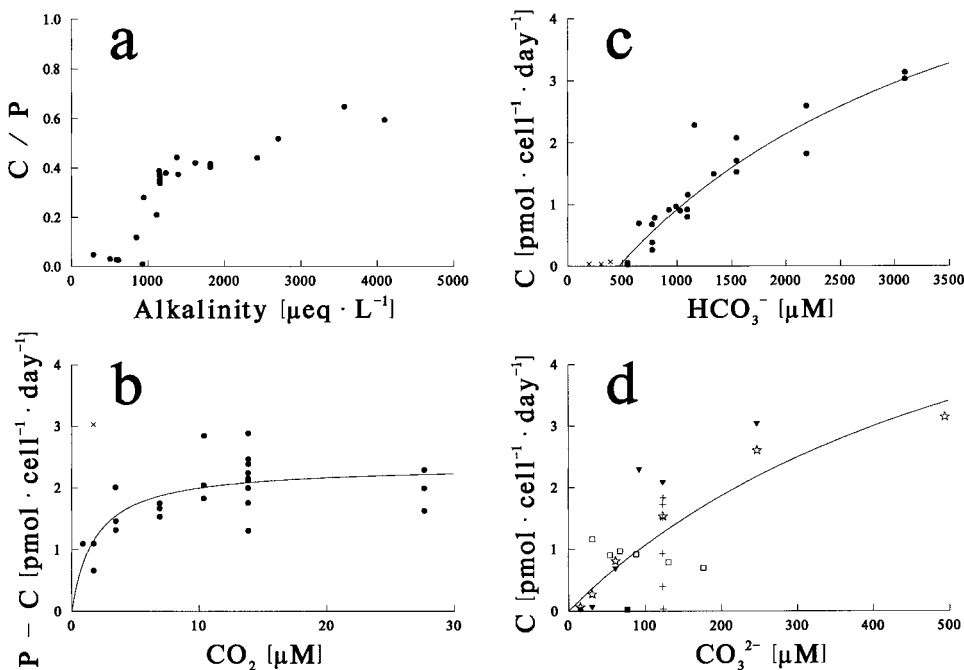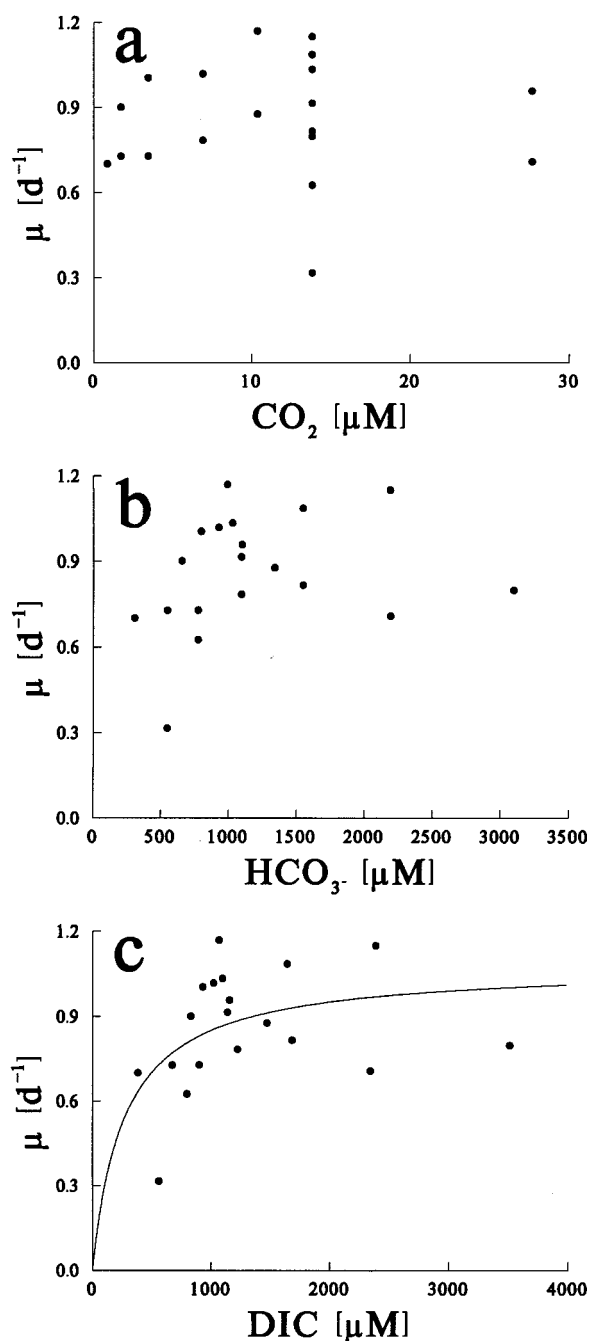
FIG. 7. Specific growth rates (μ) as a function of (a) CO_2, (b) HCO_3^-, and (c) dissolved inorganic carbon (DIC). Results of the experiments at constant CO_3^{2-}, constant alkalinity, and constant CO_2. The fitted curve is likely to depend on the experimental procedure and does not reflect the physiology of this strain of *Emiliania huxleyi* (for details, see text).

crease 16-fold (Fig. 2a). At constant CO_2, the concentration of CO_3^{2-} increases 16-fold as the HCO_3^- concentration increases fourfold (Fig. 2d). Accordingly, the calcification rate increases with the CO_3^{2-} concentration (Fig. 5c, ▼ constant pH, ☆ constant CO_2). At constant alkalinity, the CO_3^{2-} concentration increases sixfold as the HCO_3^- con-

centration decreases 1.6-fold (Fig. 2c). The concomitant decrease in calcification rate can be traced in Figure 5c (□ constant alkalinity), but because of the small change in calcification rate, this has little influence on the fit to Michaelis–Menten kinetics. This is an example of the complex equilibria within the DIC system, and it shows that conclusions about the influence of either the DIC system on C use or of C use on the DIC system need to be addressed with due caution.

As mentioned in the Results section, photosynthesis in *E. huxleyi* is proposed to depend on two sources of CO_2: an external CO_2 source in the seawater medium and an internal CO_2 source that is generated by calcification. In the experiment at constant CO_2, the external source was constant, and indeed the difference between photosynthesis and calcification was fairly constant. By plotting the remainder (the photosynthesis that is fixed from the internal source) against the calcification rate, it can be calculated that the CO_2 that is generated by calcification is used with an efficiency of 0.97 ± 0.08 (Fig. 4). Because *E. huxleyi* was grown on NO_3^- and constitutes an H^+ sink for the cell (or OH^- source; Brewer and Goldman 1976), the maximum expected efficiency is only 0.88 (at an average POC/PON ratio of 7.4). The latter consideration also indicates that the V_{max} but not $K_{1/2}$ of photosynthesis on external CO_2 (Fig. 5a) might depend on the nitrogen source.

The ratio of calcification versus photosynthesis (C/P in Fig. 3) was between 0 and 1 under all conditions tested for this strain. This means that at nutrient-saturated growth, no increase in CO_2 concentration is associated with the decrease in alkalinity due to calcification and no liberation of gaseous CO_2 from the seawater. Thus, in contrast with recent suggestions (Crawford and Purdie 1997 and references therein), during the nutrient-saturated productive phase of blooms of *E. huxleyi*, no increase in fCO_2 is to be expected. Only during the transient nutrient-limited phase is a C/P ratio greater than 1 likely to occur (Paasche 1999) with a short-lived increase in fCO_2, as was observed during a mesocosm study (Purdie and Finch 1994). In fact, from our results the expected decrease in fCO_2 is stronger than that expected from a C/P ratio of 1, which is often used as the standard ratio. This extra decrease in fCO_2 is due to the photosynthetic use of CO_2 from the seawater medium, next to the use of HCO_3^- in both photosynthesis and calcification.

It might be expected that the calcification rate would have increased at low CO_2 concentrations to generate more CO_2 for photosynthesis, but this was not found. The energy requirement of calcification should not be a factor in our experiments, as *E. huxleyi* was grown at nutrient and light saturation. Apparently, the calcification rate is dependent only on the HCO_3^- concentration and is not regulated by the

CO_2 concentration. Regulation does not seem to be required because *E. huxleyi* was able to use all the extra CO_2 that was generated under all conditions that were tested. The apparently optimal efficiency with which the protons, that are generated by calcification, are used in photosynthesis gives some indication that this is the major physiological reason, in the evolutionary sense, for *E. huxleyi* to calcify. More specifically, we suggest that the unique feature of *E. huxleyi* among coccolithophorids to continue calcification after a complete coccosphere is formed makes it possible to optimize the use of dissolved inorganic carbon. This might be the reason that it is the most successful coccolithophorid species. Whether the highly organized form in which $CaCO_3$ is precipitated and the incorporation of the coccoliths into a coccosphere constitute additional advantages for *E. huxleyi* (Young 1994) falls outside the scope of this study.

In this study it was shown that calcification allows *E. huxleyi* to efficiently use both HCO_3^- and CO_2 in photosynthesis (Fig. 6). This is also reflected in the dependence of the specific growth rate (μ) on both HCO_3^- and CO_2 (Fig. 7a, b). However, unlike μ, the rate of photosynthesis is not saturated with HCO_3^- up to a concentration of 3500 μM. This is a rather puzzling result, as the cells were adapted to the media for at least five divisions, and unbalanced growth seems rather unlikely after that time. Cells do produce DOC at high light conditions (W. Stolte, pers. comm.), but this cannot be the explanation because the rate of photosynthesis was based on ^{14}C incorporation into the particulate fraction. Moreover, the photosynthetic rate per cell was based on the same cell counts that were used to calculate the growth rates.

The conspicuous presence of *E. huxleyi* as blooms in the upper mixed layer of the temperate zones of the oceans and as coccoliths in sediments throughout the greater part of the oceans is rather surprising in view of its relatively low μ_{max} of $1.1 \cdot day^{-1}$. We have already mentioned the inconsistency between an increase in photosynthetic rates while μ is saturated with inorganic carbon. This might be a pointer toward a surplus of cell resources that might stimulate the efficient use of other resources, such as PO_4^{3-} and Zn^{2+}.

Anning, T., Nimer, N., Merrett, M. J. & Brownlee, C. 1996. Costs and benefits of calcification in coccolithophorids. *J. Mar. Syst.* 9:45–56.

Bates, R. G. 1975. pH scales for sea water. *In* Dahlem workshop on the nature of seawater. *Phys. Chem. Sci. Res. Rep.* 1:313–31.

Brewer, P. G. & Goldman J. C. 1976. Alkalinity changes generated by phytoplankton growth. *Limnol. Oceanogr.* 21:108–17.

Brown, C. W. & Yoder, J. A. 1993. Blooms of *Emiliania huxleyi* (Prymnesiophyceae) in surface waters of the Nova Scotian Shelf and the Grand Bank. *J. Plankton Res.* 15:1429–38.

——— 1994. Coccolithophorid blooms in the global ocean. *J. Geophys. Res.* 99:7467–82.

Brownlee, C., Davies, M., Nimer, N., Dong, L. F. & Merrett, M. J. 1995. Calcification, photosynthesis and intracellular regulation in *Emiliania huxleyi*. *Bull. Inst. Oceanogr. Monaco* 14:19–35.

Crawford, D. W. & Purdie, D. A. 1997. Increase of PCO_2 during blooms of *Emiliania huxleyi*: theoretical considerations on the asymmetry between acquisition of HCO_3^- and respiration of free CO_2. *Limnol. Oceanogr.* 42:365–72.

Dickson, A. G. 1981. An exact definition of total alkalinity and a procedure for the estimation of alkalinity and total inorganic carbon from titration data. *Deep Sea Res. Oceanogr., A* 28:609–23.

Egge, J. K. & Heimdal, B. R. 1994. Blooms of phytoplankton including *Emiliania huxleyi* (Haptophyta). Effects of nutrient supply in different N:P ratios. *Sarsia* 79:333–48.

Guillard, R. R. L. 1975. Culture of phytoplankton for feeding marine invertebrates. *In* Smith, W. L. & Chanley, M. H. [Eds.] *Culture of Marine Invertebrate Animals*. Plenum Press, New York, USA, pp. 29–60.

Mook, W. G., Bommerson, J. C. & Staverman, W. H. 1974. Carbon isotope fractionation between dissolved bicarbonate and gaseous carbon dioxide. *Earth Planet. Sci. Lett.* 22:169–76.

Morel, F. M. M., Reinfelder, J. G., Roberts, S. B., Chamberlain, C. P., Lee, J. G. & Yee, D. 1994. Zinc and carbon colimitation of marine phytoplankton. *Nature* 369:740–2.

Nimer, N. A., Dong, L. F., Guan, Q. & Merrett, M. J. 1995. Calcification rate, dissolved inorganic carbon utilization and carbonic anhydrase activity in *Emiliania huxleyi*. *Bull Inst. Oceanogr. Monaco* 14:43–9.

Nimer, N. A., Guan, Q. & Merrett, M. J. 1994. Extra and intracellular carbonic anhydrase in relation to culture age in a high-calcifying strain of *Emiliania huxleyi* Lohmann. *New Phytol.* 126:601–7.

Paasche, E. 1962. Coccolith formation. *Nature* 193:1094–5.

——— 1964. A tracer study of the inorganic carbon uptake during coccolith formation and photosynthesis in the coccolithophorid *Coccolithus huxleyi*. *Physiol. Plant.* 3(Suppl.):1–82.

——— 1999. Roles of nitrogen and phosphorus in coccolith formation in *Emiliania huxleyi* (Prymnesiophyceae). *Eur. J. Phycol.* (in press).

Paasche, E. & Brubak, S. 1994. Enhanced calcification in the coccolithophorid *Emiliania huxleyi* (Haptophyceae) under phosphorus limitation. *Phycologia* 33:324–30.

Purdie D. A. & Finch, M. S. 1994. Impact of a coccolithophorid on dissolved carbon dioxide in sea water enclosures in a Norwegian fjord. *Sarsia* 79:379–89.

Raven, J. A. & Johnston, A. M. 1991. Mechanisms of inorganic carbon acquisition in marine phytoplankton and their implications for the use of other resources. *Limnol. Oceanogr.* 36:1701–14.

Roy, R. N., Roy, L. N., Vogel, K. M., Porter-Moore, C., Pearson, T., Good, C. E., Millero, F. J. & Campbell, D. M. 1993. The dissociation constants of carbonic acid in seawater at salinities 5 to 45 and temperatures 0 to 45 °C. *Mar. Chem.* 44:249–67.

Sikes, C. S., Roer, R. D. & Wilbur, K. M. 1980. Photosynthesis and coccolith formation: inorganic carbon sources and net inorganic reaction of deposition. *Limnol. Oceanogr.* 25:248–61.

Sikes, C. S. & Wilbur, K. M. 1982. Functions of coccolith formation. *Limnol. Oceanogr.* 27:18–26.

Spero, H. J., Bijma, J., Lea, D. W. & Bemis, B. E. 1997. Effect of seawater carbonate chemistry on planktonic foraminiferal carbon and oxygen isotope values. *Nature* 390:497–500.

Thode, H. G., Shima, M., Rees, C. F. & Krishnamurty, K. V. 1965. Carbon-13 isotope effects in systems containing carbon dioxide, bicarbonate and metal ions. *Can. J. Chem.* 43:582.

van Bleijswijk, J., van der Wal, P., Kempers, R. & Veldhuis, M. 1991. Distribution of two types of *Emilliania huxleyi* (Prymnesiophyceae) in the northeast Atlantic region as determined

by immunofluorescence and coccolith morphology. *J. Phycol.* 27:566–70.

van Bleijswijk, J. D. L., Kempers, R. S. & Veldhuis, M. J. 1994. Cell and growth characteristics of types A and B of *Emiliania huxleyi* (Prymnesiophyceae) as determined by flow cytometry and chemical analyses. *J. Phycol.* 30:230–41.

Verardo, D. J., Froelich, P. N. & McIntyre, A. 1990. Determination of organic carbon and nitrogen in marine sediments using the Carlo Erba NA-1500 analyzer. *Deep Sea Res.* 37:157–65.

Vogel, J. C., Grootes, P. M. & Mook, W. G. 1970. Isotope fractionation between gaseous and dissolved carbon dioxide. *Zietschr. Physik* 230:225–38.

Weiss, R. F. 1974. Carbon dioxide in water and seawater: the solubility of a non-ideal gas. *Mar. Chem.* 2:203–15.

Westbroek, P., Young, J. R. & Linschooten, K. 1989. Coccolith production (biomineralization) in the marine alga *Emiliania huxleyi*. *J. Protozool.* 36:368–73.

Wolf-Gladrow, D. & Riebesell, U. 1997. Diffusion and reactions in the vicinity of plankton: a refined model for inorganic carbon transport. *Mar. Chem.* 59:17–34.

Young, J. R. 1994. The functions of coccoliths. *In* Winter, A. & Siesser, W. G. [Eds.] *Coccolithophores.* Cambridge University Press, Cambridge, pp. 63–82.